Airway obstruction in respiratory viral infections due to impaired mucociliary clearance

N Bessonov, V Volpert

Received: 25 October 2022 | Revised: 14 March 2023 | Accepted: 2 April 2023

DOI: 10.1002/cnm.3707

SPECIAL ISSUE ARTICLE

WILEY

Airway obstruction in respiratory viral infections due to impaired mucociliary clearance

N. Bessonov[1] | **V. Volpert**[2,3]

[1]Institute of Problems of Mechanical Engineering, Russian Academy of Sciences, Saint Petersburg, Russian Federation

[2]Institut Camille Jordan, UMR 5208 CNRS, University Lyon 1, Villeurbanne, France

[3]S.M. Nikolskii Mathematical Institute, Peoples Friendship University of Russia (RUDN University), Moscow, Russian Federation

Correspondence
V. Volpert, Institut Camille Jordan, UMR 5208 CNRS, University Lyon 1, 69622 Villeurbanne, France.
Email: volpert@math.univ-lyon1.fr

Funding information
RUDN University Scientific Projects Grant System

Abstract

Respiratory viral infections, such as SARS-CoV-2 or influenza, can lead to impaired mucociliary clearance in the bronchial tree due to increased mucus viscosity and its hyper-secretion. We develop in this work a mathematical model to study the interplay between viral infection and mucus motion. The results of numerical simulations show that infection progression can be characterized by three main stages. At the first stage, infection spreads through the most part of mucus producing airways (about 90% of the length) without significant changes in mucus velocity and thickness layer. During the second stage, when it passes through the remaining generations, mucus viscosity increases, its velocity drops down, and it forms a plug. At the last stage, the thickness of the mucus layer gradually increases because mucus is still produced but not removed by the flow. After some time, the thickness of the mucus layer in the small airways becomes comparable with their diameter leading to their complete obstruction.

KEYWORDS

airway obstruction, bronchial tree, mathematical modeling, mucus motion, viral infection

1 | INTRODUCTION

Severe form of COVID-19 disease can be accompanied by impaired mucociliary clearance and lung obstruction[1] due to mucus hyper-secretion and increased mucus viscosity.[2,3] Similar manifestations can be observed for influenza and some other respiratory viral diseases.[4] In this work we will develop a mathematical model describing the interplay between respiratory viral infections and mucociliary clearance in order to investigate mucus accumulation and airway obstruction.

Bronchial epithelium is covered with the airway surface liquid (ASL) which consists of periciliary layer (PCL) and mucus produced by goblet cells and submucosal glands. Coordinated motion of cilia at the surface of cilia cells moves ASL towards the pharynx.[5] Mucus protects the epithelial tissue from pathogens removing them with convective flow and neutralizing virus due to mucin molecules.[6]

SARS-CoV-2 virus can infect goblet and cilia cells and influence mucus production and motion.[7] Mucus becomes more viscous in the infected tissue due to debris of viral particles and dead infected cells.[8] Moreover, more viscous mucus is produced due to infection and inflammation.[1] In particular, SARS-CoV-2 activates mast cells which produce inflammatory cytokines IL-1β and TNF-α. Inflammation and infection of epithelial cells lead to increased concentration of mucin molecules MUC5AC and MUC5B correlating with more viscous mucus. Furthermore, viral infection and inflammation activate various pathways leading to mucus hyper-secretion.[2,3] Autopsy studies of deceased COVID-19 patients showed the presence of inflammation, increased level of mucus, more viscous mucus and mucus plugs in small airways.[1]

Viral infection spreads in cell cultures and tissues due to virus replication inside infected cells and its diffusion in the extracellular space. This infection spreading can be described as a reaction–diffusion wave.[9] A delay reaction–diffusion model for the concentration of infected cells, uninfected cells and virus allows the determination of the spreading speed and of the viral load.[10] The wave speed correlates with plaque size in virus plaque assays and with virus virulence,[11–13] while viral load in the upper respiratory tract determines virus infectivity, that is, the rate of infection transmission from infected to uninfected individuals.[14] Parameter estimation for different variants of the SARS-CoV-2 infection allows the assessment of their virulence and infectivity in agreement with the experimental, clinical and epidemiological data.[13] The basic model of infection spreading[9,10] was further developed to study the influence of immune response,[15] virus mutation and competition,[16] intracellular regulation of virus replication.[17,18]

Infection spreads in the respiratory tract from sinonasal epithelium towards alveoli.[19] This infection spreading was modeled in[20] taking into account local mucus motion in the scale of a single bronchiole. The investigation of the two-layer model (epithelial cell layer, fluid layer) showed that infection transmission downwards (against fluid flow) occurs due to virus diffusion in the cell layer, and it is weakly influenced by the flow. Indeed, if infection spreading occurred due to diffusion in the fluid layer, then ASL motion would practically stop infection progression towards the lungs in contradiction with the clinical data.[19]

Mucus is produced in 16 generations of airways from the largest one about 10 cm length and 2 cm in diameter to the smallest ones which contains about 32 thousand bronchioles with 0.16 cm length and 0.06 cm diameter. Though the mucus production rate decreases towards small bronchioles, the total mucus production increases due to their large number. Mucus moves in the direction from small to large airways, and the thickness of mucus layer gradually increases. We will use here the model of mucus motion developed in[21] for the investigation of cystic fibrosis. We will couple this model with the model of viral infection by means of variable mucus viscosity in the infected epithelial tissue.

We will show in this work that viral infection progression in the bronchial tree has three main stages. At the first stage, infection spreads along the first 11-12th generations without significant change in the thickness of mucus layer and of its velocity since the major part of mucus is produced in the last generations where its viscosity is still normal. At the second stage, infection wave passes through the last generations changing there mucus viscosity. The second stage is much shorter, since bronchiole length in the last generations is small. At the end of the second stage, mucus velocity drastically decreases due to its high viscosity. The thickness of mucus layer, though increased, remains much smaller than diameters of the corresponding airways. Finally, during the last stage, mucus forms a growing plug because it is produced but not removed. After some time, the thickness of mucus layer in the last generations becomes comparable with their diameters leading to complete airway obstruction.

The contents of the paper are as follows. We present the model in the next section. In Section 3, we begin by studying mucus motion and infection separately, and then in their interaction. We discuss the model and the results in the last section.

2 | MODEL

2.1 | Geometry of the domain

We consider 16 generations of lung airways where epithelial cells are covered with airway surface liquid composed of periciliary liquid and mucus. Coordinated motion of cilia at the surface of cilia cells provides mucus motion from generation 15 to generation 0 (Figure 1).

We consider 1D problem with the space variable $x \in [0, L]$ with positive direction from generation 0 to generation 15. 1D approximation is appropriate for this problem since mucus velocity v(x,t) is directed along the airways, and its motion in the other directions can be neglected. However, we need to take into account the total circumference in the cross-section of each bronchi generation since it determines the quantity of mucus. We denote by $w(x)$ the total width of unfolded bronchi taking into account the number of bronchioles in each generation and their diameter (Figure 1).

2.2 | Equations of mucus motion

Equations of mucus motion are derived in. Ref 31. Equation for the thickness $H(x,t)$ of the mucus layer

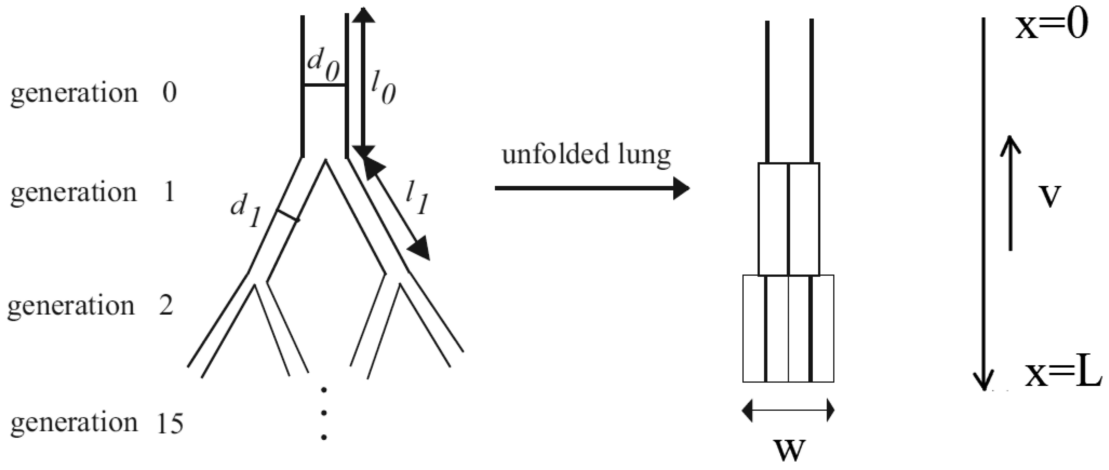

FIGURE 1 Schematic representation of 16 generations of bronchial tree with mucus motion (left) and the corresponding computational domain (right). The total width of each generation is denoted by $w(x)$, where x is the coordinate along the airways. Mucus moves in the direction of generation 0.

$$w(x)\frac{\partial H}{\partial t} = -\frac{\partial (w(x)vH)}{\partial x} + w(x)J(x) \tag{2.1}$$

is determined by the mass conservation taking into account the width of the layer $w(x)$. Its right-hand side contains convective term and mucus production term with the source density $J(x)$ depending on the space variable.

Equation for the mucus viscosity $\mu(x,t)$

$$w(x)\frac{\partial H\mu}{\partial t} = -\frac{\partial (w(x)vH\mu)}{\partial x} + D\frac{\partial}{\partial x}\left(Hw(x)\frac{\partial \mu}{\partial x}\right) + w(x)J(x)(\mu_0 U + \mu_1 I)/U_0 \tag{2.2}$$

includes in the right-hand side the convective and diffusion terms and the last term describing mucus production. It takes into account that mucus viscosity increases if it is produced in infected and inflamed epithelial tissue, as discussed in the introduction. Hence, viscosity of produced mucus can be considered as a linear combination of normal viscosity μ_0 for uninfected cells U and increased viscosity μ_1 for infected cells I.

Mucus velocity $v(x,t)$ can be expressed through its viscosity[21]:

$$v(x,t) = -\frac{k_1}{1 + k_2/\mu(x,t)} \cdot \frac{\mu_1 - \mu(x,t)}{\mu_1 - \mu_0}\,. \tag{2.3}$$

Here $\mu(x,t)$ is current viscosity at some space point x and time t, μ_0 is viscosity of mucus produced by normal cells, μ_1 viscosity of mucus produced by inflamed cells. It is suppose to be sufficiently large such that $v = 0$ if $\mu = \mu_1$.

2.3 | Equations for viral infection

We consider the epithelial cell layer in the lung airways. After replication inside infected cells, virus is expelled back to the extracellular space.[22,23] We will consider two different virus concentrations, in the cell layer (composed by cells and adjacent space) and in the fluid layer, with exchange between them. There is an important difference between these two layers because convective flow essentially influences virus concentration in the fluid layer but not in the cell layer. Equation for the concentration of uninfected cells $U(x,t)$

$$\frac{\partial U}{\partial t} = -aUV_c \tag{2.4}$$

contains in the right-hand side the term describing the rate of their infection by virus V_c in the cell layer. A similar term with sign plus describes the rate of appearance of infected cells in the equation for their concentration $I(x,t)$:

$$\frac{\partial I}{\partial t} = aUV_c - \beta I. \tag{2.5}$$

The second term in the right-hand side of this equation characterizes the rate of infected cell death. Equation for the virus concentration in the cell layer $V_c(x,t)$ takes into account the layer width $w(x)$ and its thickness h considered as a given constant:

$$w(x)h\frac{\partial V_c}{\partial t} = D_1 h\frac{\partial}{\partial x}\left(w(x)\frac{\partial V_c}{\partial x}\right) + bw(x)hI_\tau + w(x)\left(pV_f - qV_c\right) - \sigma_1 w(x)hV_c. \tag{2.6}$$

The first term in the right-hand side of this equation describes virus diffusion, then its production by infected cells with a time delay in virus replication, $I_\tau(x,t) = I(x,t-\tau)$. The next term corresponds to virus exchange between the cell and fluid layers, and the last term describes virus death. Equation for the virus concentration in the fluid layer $V_f(x,t)$

$$w(x)\frac{\partial HV_f}{\partial t} = -\frac{\partial\left(w(x)vHV_f\right)}{\partial x} + D_2\frac{\partial}{\partial x}\left(Hw(x)\frac{\partial V_f}{\partial x}\right) + w(x)\left(qV_c - pV_f\right) - \sigma_2 w(x)HV_f \tag{2.7}$$

is similar to the previous equation with added convective term and with variable layer thickness $H(x,t)$.

2.4 | Boundary and initial conditions

We consider no-flux boundary conditions for V_c, V_f and μ at $x=0$ and $x=L$. Next, $H=0$ at $x=L$, while the boundary condition at $x=0$ for this function is not imposed because the flow velocity is negative. Boundary conditions for U and I are not needed.

The initial conditions are as follows: $U(x,0)=U_0$, $I(x,0)=0$, $V_c(x,0)=V_0$ for $0\le x\le x_0$ and $V_c(x,0)=0$ elsewhere, $V_f(x,0)=0$, $\mu(x,0)=\mu_0$. Here U_0, V_0, x_0, μ_0 are some positive constants. Next, $H(x,0)=H_0(x)$, where $H_0(x)$ is the stationary layer thickness for the constant mucus viscosity μ_0.

The values of parameters and numerical implementation of the model will be presented in the appendix.

3 | RESULTS

3.1 | Mucus motion without infection

In the case without infection, solution of system (2.1)–(2.3) converges to a stationary solution with a constant viscosity μ_0 and some constant velocity v. An example of such stationary solution is shown in Figure 2.

The layer width $w(x)$ and the rate of mucus production $J(x)$ are given functions. The mucus thickness distribution $H(x)$, flow velocity v, flux $F(x)$ and viscosity μ are found as a solution of the problem. Mucus viscosity μ converges to a constant value μ_0 determined by the viscosity of mucus produced in uninfected cells. Therefore, flow velocity is also constant. We note that layer width strongly increases near the right boundary of the interval due to the large number of small bronchioles. Mucus moving from this wide part to a narrower part at the left of the interval increases its thickness $H(x)$. Mucus production rate $J(x)$ decreases from large bronchi to small bronchioles.

The distribution of mucus thickness depends on its viscosity (Figure 3). The function $H(x)$ slightly changes inside the same generation due to mucus production. It has a rapid change between the generations because of their different width $w(x)$. If mucus viscosity increases, the layer thickness also increases. However, it remains much smaller than the diameter of the corresponding airways even for the value $\mu = 0.159\ Pa\cdot s$ of the viscosity close to the maximal viscosity $\mu_1 = 0.16\ Pa\cdot s$. Indeed, the maximal value of $H(x)$ equals 0.03 cm (Figure 3), while the corresponding airway

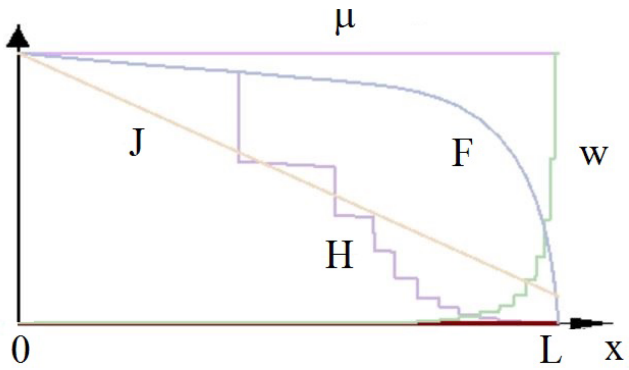

FIGURE 2 Normalized distributions of mucus thickness $H(x)$, mucus flux $F(x)$, and mucus viscosity μ (constant) for a stationary solution of system (2.1)–(2.3). Mucus production rate $J(x)$ and generation width $w(x)$ are given functions.

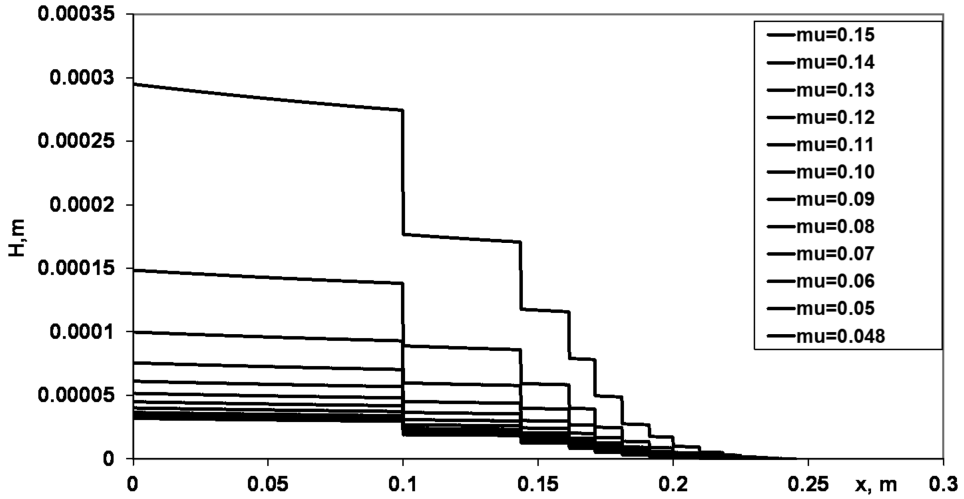

FIGURE 3 Stationary distributions of mucus thickness in consecutive bronchi generations for different values of viscosity (constant).

diameter is about 2 cm (Table A1 in Appendix). Let us note that for the maximal viscosity μ_1, the flow velocity equals 0, the stationary solution does not exist, and the thickness of layer in the model tends to infinity.

3.2 | Infection spreading

In order to describe the main properties of infection spreading, let us consider a simpler case without virus exchange between cell layer and fluid layer since it does not essentially influence the results.[20] Then its dynamics in the cell layer can be described by the system of equations

$$\frac{\partial U}{\partial t} = -aUV_c \tag{3.8}$$

$$\frac{\partial I}{\partial t} = aUV_c - \beta I, \tag{3.9}$$

$$\frac{\partial V_c}{\partial t} = D_1 \frac{\partial^2 V_c}{\partial x^2} + bI_\tau - \sigma_1 V_c. \tag{3.10}$$

In mathematical approximation, we consider this system on the whole real axis. In this case, infection progression in cell layer can be described as a reaction–diffusion wave for which the solution has the following form: $U(x,t)=u(x-ct), I(x,t)=w(x-ct), V_c(x,t)=v(x-ct)$, where c is the wave speed. It satisfies the system

$$cu'-auv=0, \tag{3.11}$$

$$cw'+auv-\beta w=0, \tag{3.12}$$

$$D_1v''+cv'+bw(\xi+c\tau)-\sigma_1 v=0, \tag{3.13}$$

where $\xi=x-ct$ and prime denotes derivative with respect to ξ, and the limits at infinity:

$$u(-\infty)=u_f,\quad u(\infty)=u_0,\quad v(\pm\infty)=w(\pm\infty)=0. \tag{3.14}$$

Here u_0 is a given value corresponding to the initial concentration of uninfected cells in the tissue, u_f is unknown value. It can be found as solution of the equation

$$ln\frac{u_f}{u_0}=R_v\left(\frac{u_f}{u_0}-1\right), \tag{3.15}$$

where $R_v=abu_0/(\beta\sigma_1)$ is the virus replication number.[10,16] It has a solution $0<u_f<u_0$ if $R_v>1$. Otherwise, such solution does not exist, and infection does not spread.

Infection progression in cell layer is characterized by the viral load $V_x=\int_{-\infty}^{\infty}v(\xi)d\xi$ and by the spreading speed c_0. Both of them can be determined analytically[10,16]:

$$V_X=\frac{c_0R_v}{a},\quad c_0=\min_{\mu>\mu_0}F(\mu),$$

where

$$F(\mu)=\sqrt{\frac{D\mu^2(\mu+\beta)}{(\mu+\sigma)(\mu+\beta)-abu_0e^{-\mu\tau}}}$$

and μ_0 is a positive zero of the denominator.

Let us note that for $\beta=0$, one of the conditions in (3.14) change to the following one: $w(-\infty)=u_0$. Furthermore, R_v and V_X are not well defined.[9] However, there exists a traveling wave solution, and its wave is given by the same expression. Furthermore, it is shown that waves exist for all values of the speed greater than or equal to the minimal speed c_0. The wave with the minimal speed c_0 is more interesting for applications since the solution of the initial boundary value problem with an initial condition with a bounded support converges to it.

In the case of a constant flow velocity v, constant mucus layer width w and thickness H, we obtain a two-layer problem (2.4)–(2.7) independent of equations of mucus motion (2.1)–(2.7). There are different regimes of infection spreading depending on the values of virus diffusion coefficients D_1 and D_2 in the cell layer and in the fluid layer, respectively. Let us recall that the cell layer includes epithelial cells and adjacent extracellular space where flow velocity is negligible. Due to the heterogeneity of this layer including cell surface, cilia and fluid, virus diffusion coefficient there is not known. Numerical simulations show that infection spreading speed against mucus flow strongly depends on the ratio of the diffusion coefficients.[20] If we assume that virus diffusion mainly occurs in the (homogeneous) fluid layer, that is, $D_1\ll D_2$, then for physiologically realistic values of mucus velocity, infection does not spread towards the lower respiratory tract (against flow), in contradiction to the clinical data. This analysis shows that the values of diffusion coefficients are of the same order, $D_1\approx D_2$. In this case, infection mainly spreads along the cell layer, while the influence of fluid flow is negligible. This conclusion allows us to consider infection spreading independently of mucus flow. On the other hand, mucus flow is influenced by infection since mucus produced in infected tissue is more viscous.

3.3 | Interaction of infection spreading and mucus motion

According to the previous section, infection spreads along the cell layer with a spreading speed weakly dependent on mucus motion. Mucus produced in the infected tissue has larger viscosity and smaller velocity. Therefore, infection propagation influences mucus motion, but the opposite influence is negligible.

Analysis of the simulations allows us to identify several main stages of infection progression in human airways. At the first stage, during which infection passes through about 12 generations, mucus flow changes weakly. When it arrives to the last generations, mucus velocity essentially decreases, it practically stops, but the thickness of the mucus layer remains close to normal. At the last stage, mucus accumulates due to its production and stagnation resulting in the airway obstruction. We now proceed to a more detailed presentation of the results.

3.3.1 | Infection progression in the first 11–12 generations

Viral infection spreads along the bronchi as a reaction–diffusion wave with a constant speed. It converts uninfected cells into infected cells. For simplicity of presentation and of the interpretation of the results, we neglect here death of infected cells ($\beta = 0$). Infected goblet cells produce more viscous mucus decreasing flow velocity. However, this effect remains sufficiently weak during the most part of infection progression.

Figure 4 shows the distribution of infected cells at the moment of time when they fill 10 generations of bronchi, which correspond to about 90% of the total length (22 cm from 24 cm). Mucus viscosity changes about twice from $0.048 Pa \cdot s$ in the remaining generations till $0.084 Pa \cdot s$ at generation 0 where viscous mucus accumulates. This relatively small change of mucus viscosity is determined by the fact that most part of it is produced in the last generations where cells are not yet infected.

Flow velocity also weakly changes from 1.1×10^{-4} m/s in the last bronchi generations till 0.82×10^{-4} m/s in the first generations. Finally, the height of the mucus layer H remains practically the same as without infection with the maximal value 4.15×10^{-5} m at the entrance of the bronchial tree (generation 0, mucus outflow), versus 3.2×10^{-5} m without infection. This small change of the mucus layer does not have significant physiological influence. Mucus layer in small bronchioli almost does not change. Thus, the first stage of infection progression does not have physiological significance from the point of view of mucus flow.

3.3.2 | Infection progression in the last generations

When infection arrives to the last generations, the changes in mucus viscosity and velocity accelerate and become more and more significant. By the moment when the whole interval is filled by infected cells, mucus viscosity reaches the values $0.13 - 0.15\ Pa \cdot s$, and its velocity changes between 1.2×10^{-5} m/s and 3.7×10^{-5} m/s, that is, it is about an order of magnitude less than at the previous stage.

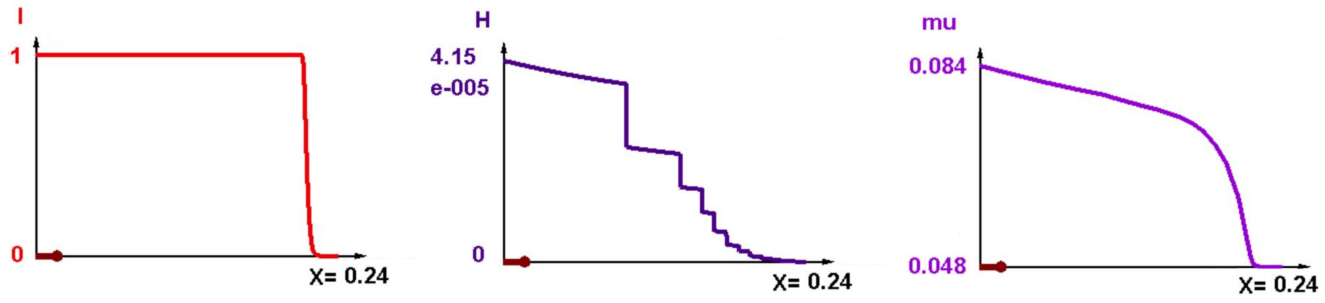

FIGURE 4 Infected cells fill about 90% of bronchi length (taken 24 cm), which corresponds to 10 generations (left). The mucus layer thickness (middle) slightly increases, but it remains orders of magnitude smaller than diameters of the corresponding airways. Mucus viscosity (right) increases approximately twice in the infected tissue. Concentration of infected cells is given in dimensionless units, interval length and layer thickness in meters, viscosity in $Pa \cdot s$.

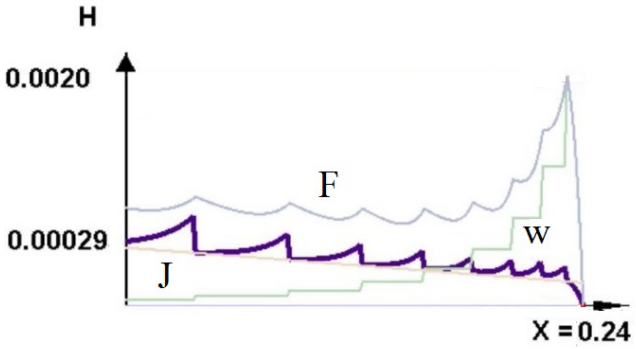

FIGURE 5 Mucus thickness distribution (bold line) in the last bronchi generations during plug growth (zoom on the last airway generations). The flux F increases towards the left, reaches the maximum and then decreases because of plug formation. Small mucus flux in large airways is determined by mucus production there. Mucus production rate $J(x)$ decreases in small airways, while the total width $w(x)$ increases.

Mucus distribution at the end of the second stage does not significantly change. Its maximal height is reached at the largest bronchus. It is about twice more than at the end of the previous stage, but it remains two orders of magnitude less than bronchus diameter. In smaller bronchi, the mucus height is at least 10 times less than their diameter.

3.3.3 | Mucus stagnation and accumulation

After the second stage, flow velocity significantly decreases and further converges to zero. In the analytical approximation, neglecting convective terms in Equations (2.1), (2.3), we obtain the equations

$$\frac{\partial H}{\partial t} = J(x)\ , \quad \frac{\partial H\mu}{\partial t} = \mu_1 J(x). \tag{3.16}$$

Combining them, we obtain the equation for mucus viscosity in the form

$$H(x,t)\frac{\partial \mu}{\partial t} = (\mu_1 - \mu)J(x). \tag{3.17}$$

The first equation in (3.16) describes linear growth of mucus height $H(x,t)$ with time due to its production. Mucus viscosity converges to its maximal value μ_1 (with which it is produced), while its velocity converges to zero according to Equation (2.3). Let us note that $\mu_1 - \mu(t) \sim 1/t$ for large time.

Growth of mucus layer is not uniform since its production decreases in smaller bronchi. However, mucus accumulation is most dangerous in the last generations where the layer thickness reaches half-diameters after some time leading to complete bronchus obstruction.

Example of numerical simulations of plug formation is shown in Figure 5. The layer thickness H has a specific wavy form with the maxima at the end of each airway generation. Since the fluid moving from the next generation backwards enters a more narrow passage ($w(x)$ is a growing function), viscous mucus is plugged there and increases layer thickness. Similar behavior can be observed for the flux F.

Time estimate of obstruction can be obtained from the equation for H. In the last generation, $J = 3 \times 10^{-10}$ m/s. For $t = 10^6$ s, we obtain $H = 3 \times 10^{-4}$ m, which is close to half-diameter of the corresponding airways and to their obstruction. This estimate of obstruction time corresponds to the simulations.

4 | DISCUSSION

Respiratory viral infections propagate along the bronchial tree as a reaction–diffusion wave. The speed of this infection wave is weakly influenced by the flow of the airway surface liquid (in the opposite direction) because virus replication

and diffusion occur in the cell layer. On the other hand, infection can essentially influence fluid flow due to increased mucus viscosity in the infected tissue and its hyper-secretion.

Numerical simulations show that there are three stages of infection progression with respect to mucus accumulation and airway obstruction. The first stage corresponds to infection progression through about first 12 generations (about 90% of the length) though this is not a precise condition. The changes of mucus viscosity, velocity and thickness remains weak because the most part of mucus is produced in the last generations which are not yet infected. Duration of this stage is determined by the speed of the infection wave. In the model, it can be determined analytically and numerically. For the values of parameters considered in this work, this stage continues about 7 days, but it can shorter for faster infection waves. Let us recall that the speed of the infection wave correlates with the virus virulence.[10,20]

The second stage is much shorter than the first one. Infection passes through the last generations during several hours. After that, all produced mucus has large viscosity, its velocity abruptly drops down, and the plus starts forming. The increase of the layer thickness is still unessential, it remains much less than diameters of the corresponding airways.

At the last stage, flow velocity is negligible, and mucus plug increases linearly in time with the speed determined by its production rate $J(x)$. Though it is smaller in the last generations, airway obstruction occurs there 6–7 days later.

This scenario of mucus accumulation and airway obstruction is generic. It can be observed for any respiratory viral infection which propagates from the upper respiratory tract to the lungs and changes mucus viscosity.

The study presented in this work has some limitations. In particular, we analyzed the effect of changing mucus viscosity, but we did not consider infection-induced increase of mucus production. We expect that moderate increase of the production rate will slightly increase the layer thickness, but it will not be essential in the case of normal viscosity. Combination of increased viscosity and production rate will accelerate plug formation and airway obstruction.

Another assumption of the model is that infection progression is uniform, that is, all airways of the same generation are infected simultaneously. However, in COVID-19 patients with lung complications, the lung damage represents about 5–10% of the total lung volume. This means that infection progresses in some airways but not in all of them. This limitation does not change the analysis and the conclusions of this work applied to the infected part of the bronchial tree.

Let us finally note that aerosol treatment, such as dornase alfa used in the case of cystic fibrosis,[21] can possibly be used for COVID-19 patients. Small liquid droplets (2–5 mkm) can penetrate up to the smallest ciliated airways and decrease mucus viscosity.[24] The distribution of aerosol droplet in the lungs is patient specific. Moreover, drug efficiency also depends on droplet distribution between obstructed and clear airways.

ACKNOWLEDGEMENTS

The last author has been supported by the RUDN University Scientific Projects Grant System, project No 025141-2-174.

CONFLICT OF INTEREST STATEMENT

The authors declare no conflict of interests.

DATA AVAILABILITY STATEMENT

Research data are not shared.

REFERENCES

1. Meyerholz DK, Reznikov LR. Influence of SARS-CoV-2 on airway mucus production: a review and proposed model. *Vet Pathol*. 2021;59 (4):1-8.
2. Shah VK et al. Overview of immune response during SARS-CoV-2 infection: lessons from the past. *Front Immunol*. 2020;11:1949. doi:10.3389/fimmu.2020.01949
3. Khan MA, Khan ZA, Charles M, et al. Cytokine storm and mucus hypersecretion in COVID-19: review of mechanisms. *J Inflamm Res*. 2021;14:175-189.
4. Keeler SP, Agapov EV, Hinojosa ME, Letvin AN, Kangyun W, Holtzman MJ. Influenza a virus infection causes chronic lung disease linked to sites of active viral RNA remnants. *J Immunol*. 2018;201:2354-2368.
5. Lee WL, Jayathilake PG, Tan Z, Le DV, Lee HP, Khoo BC. Muco-ciliary transport: effect of mucus viscosity, cilia beat frequency and cilia density. *Comput Fluids*. 2011;49:214-221.
6. Gale P. Thermodynamic equilibrium dose-response models for MERS-CoV infection reveal a potential protective role of human lung mucus but not for SARS-CoV-2. *Microb Risk Anal*. 2020;16:100140.
7. Robinot R. SARS-CoV-2 infection induces the dedifferentiation of multiciliated cells and impairs mucociliary clearance. *Nat Commun*. 2021;12:4354. doi:10.1038/s41467-021-24521-x

8. Girod S, Zahm J-M, Plotkowski C, Beck G, Puchelle E. Role of the physicochemical properties of mucus in the protection of the respiratory epithelium. *Eur Resplr J*. 1992;5:477-487.
9. Ait Mahiout L, Bessonov N, Kazmierczak B, Sadaka G, Volpert V. Infection spreading in cell culture as a reaction-diffusion wave. ESAIM. *Math Model Numer Anal*. 2022;56(3):791-814.
10. Mahiout LA, Mozokhina A, Tokarev A, Volpert V. Virus replication and competition in a cell culture: application to the SARS-CoV-2 variants. *Appl Math Lett*. 2022;133:108217.
11. Schloer GM, Hanson RP. Relationship of plaque size and virulence for chickens of 14 representative Newcastle disease virus strains. *J Virol*. 1968;2:40-47.
12. Reeve P, Poste G. Studies on the cytopathogenicity o f Newcastle disease virus: relation between virulence, polykaryocytosis and plaque size. *J Gen Virol*. 1971;11:I7-I24.
13. Peacock TP et al. The SARS-CoV-2 variant, omicron, shows rapid replication in human primary nasal epithelial cultures and efficiently uses the endosomal route of entry. *bioRxiv*. 2022;1-24. doi:10.1101/2021.12.31.474653
14. Marc A et al. Quantifying the relationship between SARS-CoV-2 viral load and infectiousness. *eLife*. 2021;10:e69302. doi:10.7554/eLife.69302
15. Ait Mahiout L, Mozokhina A, Tokarev A, Volpert V. The influence of immune response on spreading of viral infection. *Lobachevskii J Math*. 2022;43(10):2463-2476.
16. Ait Mahiout L, Kazmierczak B. Viral infection spreading and mutation in cell culture. *G V Volpert Math*. 2022;10:256. doi:10.3390/math10020256
17. Tokarev A, Mozokhina A, Volpert V. Competition of SARS-CoV-2 variants in cell culture and tissue: wins the fastest viral autowave. *Vaccines*. 2022;10(7):995.
18. Bessonov N, Bocharov G, Mozokhina A, Volpert V. Viral infection spreading in cell culture with intracellular regulation. *Mathematics*. 2023;11:1-23.
19. Bridges JP, Vladar EK, Huang H, Mason RJ. Respiratory epithelial cell responses to SARS-CoV-2 in COVID-19. *Thorax*. 2022;77:203-209. doi:10.1136/thoraxjnl-2021-217561
20. Ait Mahiout L, Bessonov N, Kazmierczak B, Volpert V. Mathematical modeling of respiratory viral infection and applications to SARS-CoV-2 progression. *Math Methods Appl Sci*. 2022; 46:1740-1751.
21. Kurbatova P, Bessonov N, Volpert V, et al. Model of mucociliary clearance in cystic fibrosis lungs. *J Theor Biol*. 2015;372:81-88.
22. Sims AC, Baric RS, Yount B, Burkett SE, Collins PL, Pickles RJ. Severe acute respiratory syndrome coronavirus infection of human ciliated airway epithelia: role of ciliated cells in viral spread in the conducting airways of the lungs. *J Virol*. 2005;79(24):15511-15524.
23. Con Y, Ren X. Coronavirus entry and release in polarized epithelial cells: a review. *Rev Med Virol*. 2014;24:308-315.
24. Gerrity TR, Lee PS, Hass FJ, Marinelli A, Werner P, Lourenço RV. Calculated deposition of inhaled particles in the airway generations of normal subjects. *J Appl Physiol*. 1979;47(4):867-873.

How to cite this article: Bessonov N, Volpert V. Airway obstruction in respiratory viral infections due to impaired mucociliary clearance. *Int J Numer Meth Biomed Engng*. 2023;e3707. doi:10.1002/cnm.3707

APPENDIX A

A.1 | NUMERICAL IMPLEMENTATION AND PARAMETERS

The system of Equations (2.1)–(2.7) was solved numerically using the finite volume method (like a conservative subversion of finite difference method). A non uniform finite difference mesh in X direction was introduced, consisting of N nodes. Each node i $(i=1,...N)$ of the mesh was assigned with a finite volume v_i. Corresponding to system (2.1)–(2.7) unknown nodal variables U_i, V_{ci}, V_{fi}, I_i were introduced.

The Equations (2.1)–(2.7) were integrated over the indicated volumes v_i. Then subsequent finite difference approximation of U_i, V_{ci}, V_{fi}, I_i to the obtained equations makes it possible to obtain a conservative stable implicit finite difference scheme that provides a solution to the problem even for the case where $w(x)$ is a discontinuous function. A similar approach was used in[21] for the model of mucus motion without infection.

The basic set of parameters is as follows:

$L=0.24$ m, $h=0.001$ m, $\mu_0=0.048$ Pa s, $\mu_1=0.16$ Pa s, $J(x)$ from 3×10^{-10} m/s to 3×10^{-9} m/s (linear function), $D_1=D_2=10^{-9}$ m^2/s, $a=3\times10^{-8}$ 1/(s virus), $b=30$ virus/(s cell), $\beta=0$ 1/s, $\sigma_1=0.0003$ 1/s, $\sigma_2=1$ 1/s, $k_1=1.4810^{-4}$ m/s, $k_2=0.0169$ Pa s.

The values of parameters are taken from[21] for the mucus flow submodel and from[10,20] for the infection submodel (some units are modified).

A.2 | BRONCHI GENERATIONS

TABLE A1 Characteristics of human airways in different generations

Generation number	Bronchus length, cm	Bronchus diameter, cm	Number of bronchi
1	10	2.01	1
2	4.36	1.56	2
3	1.78	1.13	4
4	0.965	0.827	8
5	0.995	0.651	16
6	1.01	0.574	32
7	0.890	0.435	64
8	0.962	0.373	128
9	0.867	0.322	256
10	0.667	0.257	512
11	0.556	0.198	1024
12	0.446	0.156	2048
13	0.359	0.118	4096
14	0.275	0.092	8192
15	0.212	0.073	16,384
16	0.168	0.060	32,768